DOI: 10.1002/chem.201102322

Responsive Vesicles from the Self-Assembly of Crystalline-Coil Polyferrocenylsilane-*block*-Poly(ethylene Oxide) Star-Block Copolymers

Felix H. Schacher,*[a, b] Johannes Elbert,[b] Sanjib K. Patra,[b] Siti F. Mohd Yusoff,[c] Mitchell A. Winnik,[d] and Ian Manners[b]

Abstract: We demonstrate the synthesis and characterization of star-shaped crystalline-coil block copolymers with four arms consisting of an inner block of poly(ethylene oxide) and an outer semicrystalline compartment of poly(ferrocenyldimethylsilane), $[PEO_{50}$-*b*-$PFDMS_{35}]_4$. The materials were synthesized by transition-metal-catalyzed ring-opening polymerization of dimethylsila[1]ferrocenophane in the presence of silane-functionalized four-arm PEO stars as macroinitiators and they exhibited a moderate polydispersity (PDI≅1.4). Self-assembly in mixtures of THF and different alcohols as selective solvents for the PEO block resulted in the formation of semicrystalline vesicles (ethanol, 1-butanol) or large, rather ill-defined, spherical structures (methanol). Further, both the rate of addition of the selective co-solvent and the overall solvent/non-solvent ratio drastically affected the size and stability of the self-assembled particles. We could also show that a photoacid generator, as a model for an active substance, can be encapsulated and the UV-induced generation of HCl resulted in a straightforward degradation of the organometallic vesicles.

Keywords: self-assembly · block copolymers · nanostructures · solvent effects

Introduction

The self-assembly of block copolymers has attracted intense interest over the past few decades.[1–4] Substantial progress in different fields of polymer synthesis[5–7] as well as the development of functional monomers bearing inherent triggers to change conformation or polarity upon the application of simple external stimuli have led to a broad variety of responsive systems[8] with different morphologies in the bulk, in thin films, and in solution.[9,10] Commonly exploited stimuli in solution include pH, temperature,[11] counter-ion valency, or light,[12] and more recently, redox reactions have also been reported to induce micellization.[13,14] In general, it is desirable to create systems in which conformational or morphological changes are reversible, but this often requires highly dynamic building blocks. Such dynamics in amorphous systems are often achieved by the use of low glass-transition temperatures or, in the case of polyelectrolytes, the ionic strength or salinity of the surrounding medium.[15,16]

In recent years several groups have reported on self-assembly phenomena with crystalline-coil block copolymers in which solvent quality and temperature play important roles.[17–24] We have established that where the core of a micelle is crystalline, epitaxial growth processes can be exploited to create a variety of well-defined supramolecular structures. For example, polyferrocenylsilane (PFS)-based systems with a crystalline PFS core allow the formation of monodisperse cylinders of controlled length, block co-micelles, and hierarchical architectures with spatially defined functionality by crystallization-driven living self-assembly.[17,21,22,25]

Compared with linear systems, star-shaped block copolymers are far less often investigated. The solution behavior of poly(methyl methacrylate)-*block*-poly(acrylic acid) (PMAA-*b*-PAA) systems with four[26] or eight[27] arms, as well as four-arm poly(acrylic acid)-*block*-polystyrene (PAA-*b*-PS) star-shaped block copolymers in which PS serves either as the inner[28] or outer[29] hydrophobic block, has been studied in selective solvents. Very recently, the synthesis of dendritic stars with blocks of polyglycidol and poly(*tert*-butyl glycidyl ether) has been demonstrated.[30] Synthetically most often more demanding than block structures, the preparation and aggregation of responsive star-shaped μ-[31] and hetero-arm[32] structures have also been pursued.

[a] Prof. Dr. F. H. Schacher
Institute of Organic and Macromolecular Chemistry
and Jena Center for Soft Matter (JCSM)
Friedrich-Schiller-University Jena
Humboldtstraße 10, 07743 Jena (Germany)
E-mail: felix.schacher@uni-jena.de

[b] Prof. Dr. F. H. Schacher, J. Elbert, Dr. S. K. Patra, Prof. Dr. I. Manners
School of Chemistry, University of Bristol
Bristol, England BS8 1TS (UK)
E-mail: ian.manners@bristol.ac.uk

[c] S. F. Mohd Yusoff
Universiti Kebangsaan Malaysia
43600 UKM Bangi, Selangor (Malaysia)

[d] Prof. Dr. M. A. Winnik
Department of Chemistry, University of Toronto
80 St. George Street, Toronto, Ontario, M5S 3H6 (Canada)

Supporting information for this article is available on the WWW under http://dx.doi.org/10.1002/chem.201102322. It contains additional NMR, light scattering, AFM, and TEM data.

Results and Discussion

In this contribution we report studies of the solution self-assembly of star-shaped amphiphilic PFS-based block copolymers. There is a growing amount of work on linear block copolymers that undergo crystallization-driven formation of 1D elongated objects such as cylinders,[21,23,33–35] scarves,[25] and platelets.[36,37] However, if several PFS chains are covalently bound to a central branch point, additional effects during crystallization-induced self-assembly resulting from limitations on conformational and spatial freedom can be anticipated.[38,39] We therefore targeted a star-shaped block copolymer in which the "outer" block consists of semicrystalline poly(ferrocenyldimethylsilane) (PFDMS)[40] and the "inner" block is derived from poly(ethylene oxide) (PEO). Such a material would be extremely challenging to prepare by living anionic polymerization methods, especially as effective crossover from PFS to PEO has not been readily achieved. We therefore utilized an alternative synthetic method involving metal catalysis. Although this procedure leads to materials that are structurally less perfectly defined and the control over the molecular weight is limited, it has the major advantage of allowing complex architectures to be built up very conveniently and rapidly under less experimentally rigorous conditions and with the possibility of easy scaleup.[41,42]

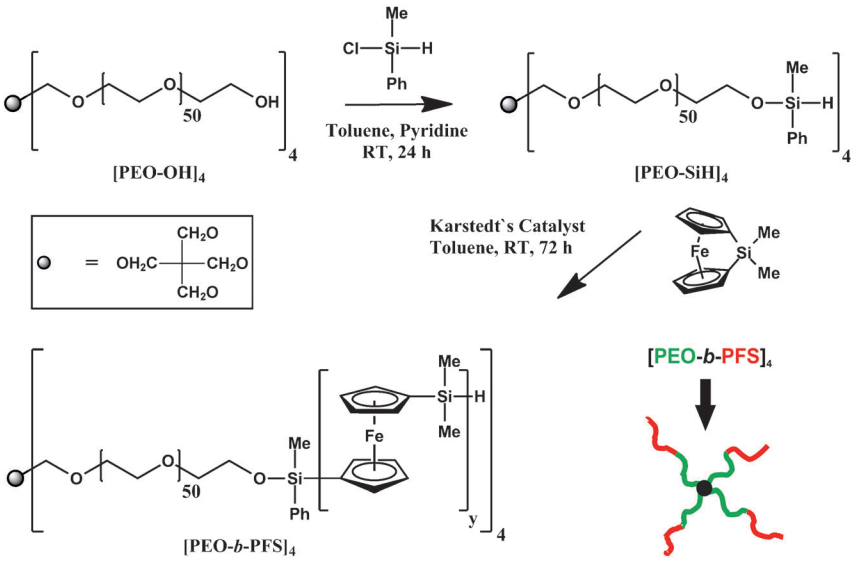

Scheme 1. Synthesis of $[(PEO_{50}\text{-}b\text{-}PFDMS)]_4$ star-block copolymers.

As a core we employed a commercially available four-arm PEO star with terminal hydroxy groups that we transformed into a suitable star macroinitiator. The use of silanes as molecular-weight mediators for the transition-metal-catalyzed ring-opening polymerization (ROP) of [1]ferrocenophane monomers and for the facile preparation of different star, graft, and block polyferrocene architectures has been demonstrated previously.[41] Moreover, the use of silane-end-functionalized PEO macroinitiators has allowed PEO-*b*-PFS diblock copolymers to be obtained.[43] We used a combination of both approaches for the preparation of star-shaped PEO-*b*-PFS block copolymers (Scheme 1).

First, the hydroxyl-terminated $[(PEO_{50})\text{-}OH]_4$ precursor was functionalized with methyl(phenyl)chlorosilane and the product was subsequently used as a star macroinitiator for the ROP of [1]ferrocenyldimethylsilane using Karstedt's catalyst ($[Pt_2(divinyltetramethyldisiloxane)_3]$). The properties of PFS homopolymers depend strongly on the substituents present at silicon: Symmetrically substituted materials are, in general, semicrystalline[24,44,45] whereas PFSs with two different substituents are amorphous.[46] The polymerization of the organometallic monomer was carried out for 72 h and, after two-fold reprecipitation of the resulting orange materials to remove any unreacted PEO star macroinitiator, a four-arm star-block copolymer with a moderate PDI was obtained. Size exclusion chromatography (SEC) traces are shown in Figure 1 and the molecular weight and compositional data are summarized in Table 1.

Metal-catalyzed ROP under such conditions is known to lead to PDIs in the range of 1.5–2 even for linear polymers.[47] Moreover, the presence of multiple silane moieties on a single macroinitiator and the detection of traces of

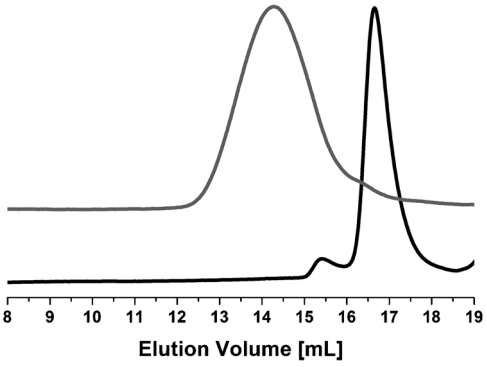

Figure 1. SEC traces of the $[PEO_{50}]_4$ precursor (black) and the $[PEO_{50}\text{-}b\text{-}PFDMS_{35}]_4$ star-block copolymer (grey) using THF and additional tetra-*n*-butylammonium bromide (0.25 wt%) as eluent.

Table 1. Characteristics of the used star polymers.

Sample	M_n [g mol^{-1}]	PDI[a]	DP_{PEO}[a]	DP_{PFS}[b]	[DP] ratio[b]
$[PEO_{50}]_4$	8800[c]	1.08	50	–	–
$[PEO_{50}\text{-}b\text{-}PFDMS_{35}]_4$	42700[b]	1.45	50	35	1.4:1

[a] Measured by SEC in THF vs. polystyrene calibration. [b] Determined by ^{1}H NMR measurements. [c] Determined by triple detection SEC in THF.

lower-molecular-weight products by SEC (Figure 1) suggested that, in addition to the four-arm star, the presence of small amounts of star-block copolymers with a lower number of arms is likely as contaminants in the purified material. However, ^{29}Si and ^{1}H NMR analyses of $[PEO_{50}$-*b*-$PFDMS_{35}]_4$ did not reveal any unreacted silane moieties (Figure S1).

Self-assembly of the $[PEO_{50}$-*b*-$PFDMS_{35}]_4$ star-block copolymer was induced through the addition of a selective solvent (EtOH) for the PEO block to dilute solutions of the material in THF (1 gL^{-1}), a common solvent for both blocks. Direct dissolution in the selective solvent or the solvent mixture was not possible, although this is a standard procedure for the preparation of uniform micelles from linear block copolymers like, for example, PFDMS-*b*-PDMS or PI-*b*-PFDMS in alkane solvents[21] or PFDMS-*b*-P2VP in isopropanol.[22] Even after heating in THF/EtOH mixtures, the star-block copolymer remained insoluble. After addition of EtOH (THF/EtOH, 1:2, v/v) to a solution in THF, the sample became slightly opaque, which indicated the formation of aggregates. Spherical vesicles with diameters of 100–200 nm were identified by transmission electron microscopy (TEM) (Figure 2A, higher magnification 2B). A thin, dark

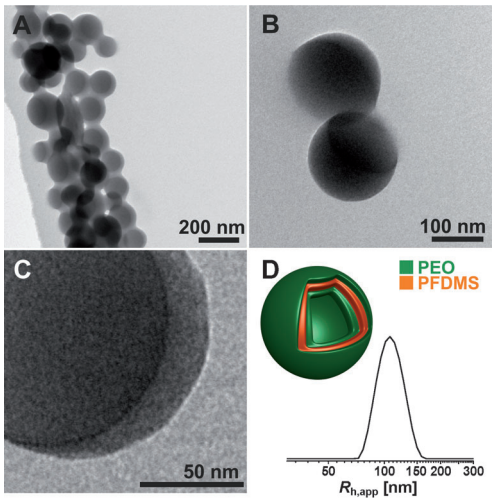

Figure 2. A) TEM micrograph of $[PEO_{50}$-*b*-$PFDMS_{35}]_4$ block copolymer vesicles from mixtures of THF/EtOH (1:2, v/v). B) and C) Increased magnifications of the image in shown in A). D) Proposed solution structure and DLS CONTIN plot at 90° in EtOH ($c = 0.066$ gL^{-1}), $R_{h,app} \cong 105$ nm.

capsule wall of 2–3 nm thickness could be distinguished (Figure 2C) and is presumably formed by the insoluble PFDMS block, whereas PEO serves as a corona and stabilizes the vesicles in solution. Remarkably, the aggregates retain their spherical shape and do not collapse, a feature attributed to the rigidity of the PFDMS wall. Only slightly collapsed vesicles were detected (Figure 2B,C). The proposed structure in solution is depicted in Figure 2D and the size by TEM was shown to be consistent with that determined by dynamic light scattering (DLS; $R_{h,app} \cong 105$ nm, 2D).

More detailed light scattering investigations are shown in Figure 3. The apparent hydrodynamic radii are constant in the range of 100–110 nm for concentrations in ethanol from

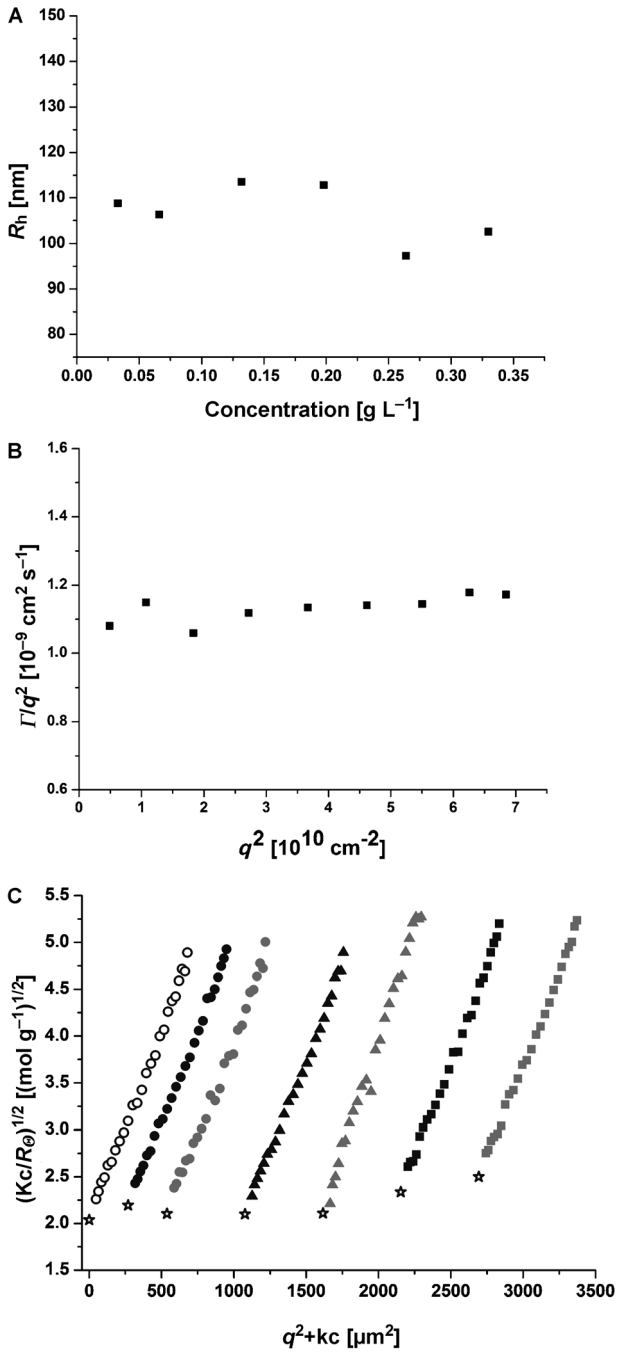

Figure 3. A) Hydrodynamic radii at a scattering angle of 90° of $[PEO_{50}$-*b*-$PFDMS_{35}]_4$ vesicles in ethanol at different concentrations. B) Reduced decay rate, Γ/q^2 versus q^2, indicating a spherical shape of the particles. C) Berry plot for six concentrations in ethanol; from SLS, $R_g = 94$ nm, $M_w = 2.11 \times 10^7$ g mol^{-1}, $N_{agg} = 494$, and $A_2 = 2.04 \times 10^{-8}$ mol dm^3 g^{-2} were obtained; here, R_θ is the Rayleigh ratio, K is a constant including the refractive index increment (dn/dc), c is the concentration, and k represents a scaling constant; key: ○: $c \to 0$; ●: $c = 0.033$ gL^{-1}; ●: $c = 0.066$ gL^{-1}; ▲: $c = 0.1321$ gL^{-1}; ▲: $c = 0.198$ gL^{-1}; ■: $c = 0.264$ gL^{-1}; ■: $c = 0.330$ gL^{-1}; ☆: $\theta \to 0$.

0.01 to 0.33 $g\,L^{-1}$ (Figure 3A). Further, angular scattering experiments confirmed a spherical shape of the aggregates, as shown by plotting the reduced decay rate, Γ/q^2, versus q^2 (Figure 3B). We also performed static light-scattering experiments in ethanol. From those, values for the radius of gyration ($R_g = 94$ nm), the molecular weight ($M_w = 2.11 \times 10^7\,g\,mol^{-1}$), and the second virial coefficient ($A_2 = 2.04 \times 10^{-8}\,mol\,dm^3\,g^{-2}$) were obtained. According to the molecular weight determined by static light scattering (SLS), the aggregation number is $N_{agg} = 494$ and the ratio of $R_g/R_h = 0.89$, which is higher than the theoretical value for a hard sphere (0.775) and close to the expected ratio for a hollow structure[48] (ca. 1.0; Figure 3C).

Following the initial self-assembly process in THF/EtOH, the vesicles could be transferred to pure EtOH and, finally, to water by dialysis. Both in THF/EtOH and in water, cryo-TEM allowed for quasi in situ visualization of the unperturbed vesicles (Figure 4).[49,50] Whereas most literature examples deal with cryo-TEM in aqueous solution,[15] there are few examples of such experiments in organic solvents or solvent mixtures, as shown for toluene[51] and dioxane/THF.[52] Both in THF/EtOH (Figure 4A) and in water (Figure 4B), spherical structures with diameters of 100–200 nm can be seen. Although, in both cases, the capsule wall was not detected, the central region of the vesicles appears darker in aqueous environment. In the latter case, some examples for fusion processes occurring between individual vesicles were also observed, as highlighted by the dashed circle in the lower part of Figure 4B. The uncollapsed nature of the vesicles was confirmed by AFM. Height profile analysis showed the presence of a majority of objects possessing comparable heights and widths consistent with a rigid structure. (Figure S2).

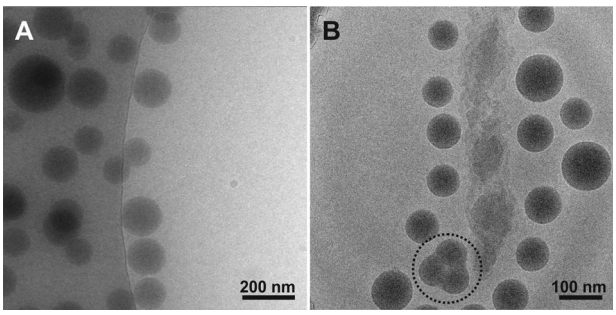

Figure 4. Cryo-TEM micrographs of $[PEO_{50}$-*b*-$PFDMS_{35}]_4$ vesicles in A) THF/EtOH 1:2 (v/v) and B) water (the dashed circle shows three individual structures fusing); the concentration in both cases was 0.33 $g\,L^{-1}$.

The formation of capsules with a size distinctly larger than the dimensions of the star-block copolymer unimers in THF ($R_{h,app} = 6.8$ nm, Figure S3A) was unexpected as the folding of several PFDMS chains into the vesicle wall would be anticipated to induce substantial curvature to the interface with the PEO core. Furthermore, we found that the attempted direct preparation of such aggregates in THF/H_2O mixtures resulted in ill-defined, porous objects (Figure S4). We therefore investigated the formation mechanism in more detail by varying the following parameters: the non-solvent that is added, the rate of addition of the non-solvent, and the common solvent/selective solvent ratio (Figure 5). As selective solvents we chose MeOH (more polar) and *n*BuOH (less polar) as alternatives to EtOH. When MeOH was used (THF/MeOH, 1:2, v/v), the resulting structures were found to be less rigid, an increased tendency for fusion was detected (see Figure 5A (TEM) and 5B (SEM)), and precipitation occurred within several hours. In Figure 5B, the formation of elongated objects with widths similar to the diameter of the single capsule is particularly evident. Here, no capsule wall could be observed by TEM and hence the structures could also be interpreted as large compound micelles, for example, as observed for amphiphilic diblock copolymers with highly asymmetric volume fractions in an aqueous environment using poly(acrylic acid) (PAA) as the hydrophilic block and polybutadiene (PB)[53] or polystyrene (PS) as the hydrophobic block.[54] In the case of *n*BuOH addition (THF/*n*BuOH, 1:2, v/v, Figure 5C), stable particle dispersions were obtained with smaller dimensions than those formed in THF/EtOH, but with a detectable capsule wall (inset in Figure 5C; for DLS, see Figure S3B (MeOH) and Figure S3C (*n*BuOH)). Presumably, as MeOH is a poorer solvent for PFDMS than higher alcohols, this decreases the amount of swelling and crystallization of the PFDMS domains. The reduced stability observed for the aggregates in THF/MeOH and the occurrence of elongated objects detected by TEM and SEM suggest that particle fusion occurs. We tentatively attribute this to a reduced crystallinity and rigidity under these conditions. This is consistent with observations made previously for the self-assembly of PFDMS-*b*-P2VP diblock copolymers in different alcohols.[22]

We also varied the rate of addition of the selective solvent EtOH from 1 min up to 2 h by using a syringe pump. Rather rapid precipitation was observed for addition periods of 20 min or longer, whereas stable colloidal dispersions were formed for an addition time of up to 15 min. However, both the turbidity (Figure 5D) and the aggregate size (Figure 5E) increased with decreasing rate of addition. We attribute this to an increased influence of the PFDMS crystallization on the self-assembly process with slower rates of addition. This resulted in the formation of larger aggregates with less curvature, as illustrated by the formation of giant particles (Figure 5G) or the formation of platelets protruding from the capsules (Figure 5H, the inset shows a single platelet at higher magnification). Furthermore, the amount of non-solvent added was also found to influence the aggregation process. For THF/EtOH (1:1, v/v), again giant structures similar to large compound micelles were obtained (SEM, Figure 5F), whereas higher ratios of EtOH resulted in capsules with decreasing size (THF/EtOH 1:1.5, $R_{h,app} = 140$ nm, Figure 5I; 1:4, $R_{h,app} = 95$ nm, Figure 5J; DLS Figure S3D) and comparable structural features as shown in Figure 2. As the volume fraction of PFDMS is rather high (87% for $[PEO_{50}$-*b*-$PFDMS_{35}]_4$), we also synthesized two star-block copolymers with lower degrees of polymerization of the semicrys-

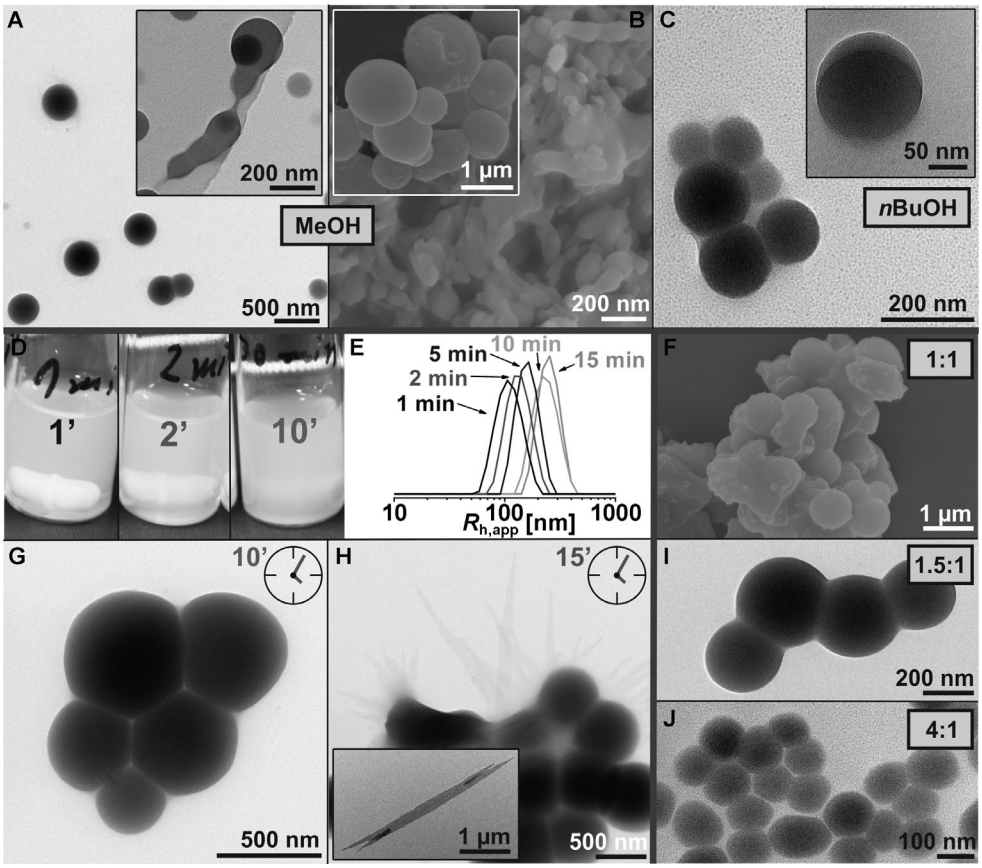

Figure 5. A) TEM micrograph of $[PEO_{50}$-*b*-$PFDMS_{35}]_4$ vesicles prepared in THF/MeOH v/v 1:2 (the inset shows the fusion of several structures). B) SEM of the precipitate occurring (the inset shows several large vesicles at higher magnification). C) TEM of vesicles prepared in THF/*n*BuOH v/v 1:2 (the inset shows a single particle with the thin dark capsule wall at higher magnification). D) Photograph and E) DLS CONTIN plots of vesicle solutions prepared by means of slow addition of EtOH with a syringe pump, both size and turbidity increase with decreasing addition speed. F) SEM of large vesicles formed at THF/EtOH v/v 1:1. G) TEM micrograph of aggregates formed when the addition of EtOH was performed over 10 min. H) TEM micrograph of particles formed for 15 min addition time; the inset shows a PFDMS platelet formed during this time. I) SEM of aggregates formed at THF/EtOH v/v 1:1.5. J) SEM of aggregates formed at THF/EtOH v/v 1:4.

talline outer block, $[PEO_{50}$-*b*-$PFDMS_{30}]_4$ and $[PEO_{50}$-*b*-$PFDMS_{16}]_4$. In both cases, initial self-assembly studies performed with mixtures of THF/EtOH resulted in structures comparable to those observed for $[PEO_{50}$-*b*-$PFDMS_{35}]_4$ with particle diameters in the range of 150–250 nm (DLS and TEM). For example, a TEM micrograph obtained for $[PEO_{50}$-*b*-$PFDMS_{16}]_4$ from THF/EtOH (1:2, v/v) is shown in Figure 6; a single object in which the capsule wall is visible is shown in the inset of Figure 6B.

Based on the results presented so far, the self-assembly process appears to proceed sufficiently fast in the early stages to prevent extensive crystallization of the PFDMS. However, once the capsules have been formed, our studies suggest that rigidity induced by crystallization of the PFDMS domains is beneficial to their stability. Indeed, WAXS analysis confirmed that the vesicles are semicrystalline (Figure 7). The diffractogram of the dried vesicles (line 3) shows several reflections that were assigned to either PFDMS or the PEO precursor (line 1, see also table in Figure 7). Furthermore, two additional reflections ($2\theta = 7.3$ and 12.15°) appear, both very sharp and intense. The *d* spacing (1.21 nm) of the most intense reflection at $2\theta = 7.3°$ is approximately twice the distance reported for the Fe–Fe vector in a linear pentamer model of PFDMS.[55] For com-

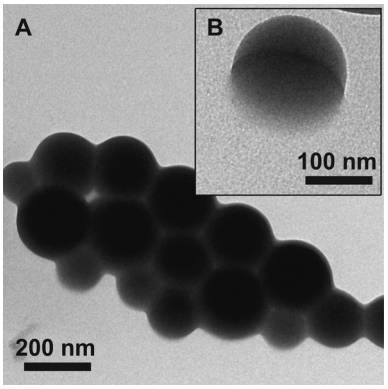

Figure 6. A) TEM micrograph of $[PEO_{50}$-*b*-$PFDMS_{16}]_4$ vesicles from THF/EtOH (1:2, v/v). B) The inset shows a single particle at higher magnification.

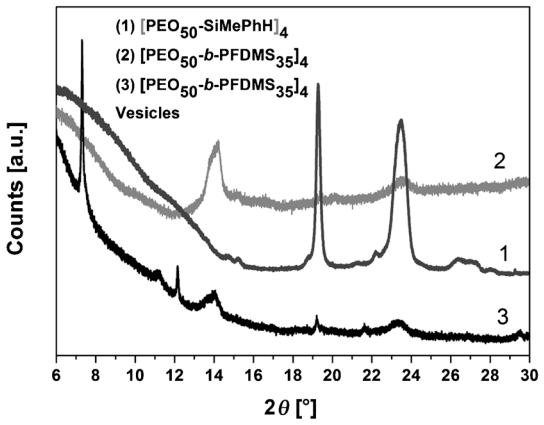

2θ[°]	d [nm]	Source
7.30	1.21	PFDMS
12.15	0.73	PFDMS
13.98	0.63	PFDMS
19.20	0.46	PEO
21.62	0.41	PFDMS
23.39	0.38	PEO
29.51	0.30	PFDMS

Figure 7. WAXS diffractograms for the $[PEO_{50}$-*b*-$PFDMS_{35}]_4$ star-shaped block copolymer (2), the vesicles after drying (3) and the PEO precursor (1); the table lists all reflections and the corresponding *d*-spacings.

parison, we also performed WAXS analysis on the star-shaped block copolymer in the bulk, prior to self-assembly (line 2, Figure 7). In this case, only the characteristic reflection at $2\theta = 13.98°$ ($d = 0.63$ nm), which corresponds to the crystalline PFDMS domains, was found.[44] This rather broad reflection was also detected for the vesicles. However, the signals at $2\theta = 7.3$ and 12.15° cannot be assigned to linear PFDMS, PEO, or the $[PEO_{50}$-*b*-$PFDMS_{35}]_4$ diblock copolymer prior to vesicle formation. It might be that the curvature induced through the capsule wall leads to an increase in the Fe–Fe distance for PFDMS.[56] We also tried to confirm these observations by selected area electron diffraction (SAED) measurements in TEM. Unfortunately, the crystalline capsule wall seems to be rather sensitive to the incident electron beam and no distinct diffraction signals could be observed.

The $[PEO_{50}$-*b*-$PFDMS_{35}]_4$ vesicles combine two advantageous and valuable properties: First, vesicles in general can be used to encapsulate and protect species of interest[57,58] and, secondly, the capsule wall is redox-responsive, owing to the electrochemical characteristics of PFDMS.[24,59] With the aim of exploiting the sensitivity of PFDMS towards acids, which leads to cleavage of the main chain, we incorporated a photoacid generator (PAG), 2-(4-methoxystyryl)-4,6-bis-(trichloromethyl)-1,3,5-triazine, by dissolution of both the star-block copolymer and the PAG in THF (mass ratio 1:1) followed by subsequent addition of EtOH (Figure 8). During vesicle formation, a certain amount of PAG should be trapped inside the capsules. The remaining free PAG was removed by five successive dialysis steps against EtOH (for TEM of the vesicles with encapsulated PAG see Supporting Information, Figure S5). Next, UV irradiation was used to induce the decomposition of the PAG with the formation of HCl,[60] and the subsequent cleavage of the $[PEO_{50}$-*b*-$PFDMS_{35}]_4$ aggregates into soluble fragments was indicated by subsequent SEC analysis of the products (Figure S6). A change in turbidity can be readily detected (Figure 8A) and DLS confirmed the destruction of the vesicles. The controlled disassembly of nanostructures through external triggers is desirable, as recently shown for the oxidative[61] or mechanical[62] decomposition of polymersomes. Our approach with a PAG is, however, an irreversible process.

We also attempted to partially oxidize the PFDMS vesicle wall by using different chemical oxidants in the THF/EtOH (1:2, v/v) mixture (Figure 8B). It has been shown earlier that the walls of hollow PFS-based microcapsules can be rendered porous through controlled oxidation processes.[63] In our case, even when using bulky counter ions like $[SbF_6]^-$, partial oxidation always resulted in the decomposition of the vesicle wall. This is illustrated in the TEM micrograph

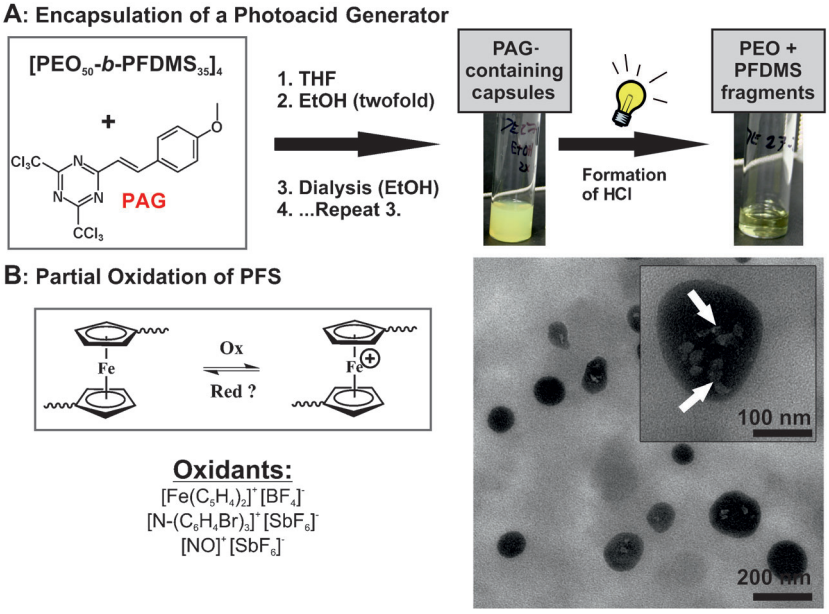

Figure 8. A) Encapsulation of a PAG into $[PEO_{50}$-*b*-$PFDMS_{35}]_4$ vesicles and removal over several dialysis steps, subsequent UV irradiation of the turbid yellow solution (TEM of vesicles after five dialysis steps is shown in Figure S5) leads to decomposition of PFDMS and the dissolution of the capsules, visible through the clear yellow solution obtained. B) Partial oxidation of PFDMS with different oxidation agents and resulting degradation of the PFDMS capsule wall, indicated by the two white arrows in the inset.

in Figure 8B for the oxidation with 0.25 equiv of $[N(C_6H_4Br)_3]^+[SbF_6]^-$. Clearly, holes were generated and the capsules then became unstable and precipitation was observed.

Conclusion

In summary, self-assembly of $[PEO_{50}$-*b*-$PFDMS_{35}]_4$ star-block copolymers with a semicrystalline PFDMS outer block in mixtures of THF and different alcohols, surprisingly, resulted in the formation of spherical structures. If ethanol was used as the selective co-solvent and for appropriate solvent/non-solvent ratios, the formation of crystalline vesicles could be demonstrated by TEM and light scattering techniques. In other cases, for example, for methanol or for THF/ethanol ratios lower than 1:2 (v/v), structures similar to earlier reported large compound micelles were found.[53,54] To our knowledge, this behavior has not been reported for star-shaped block copolymer systems before. Although at this preliminary stage it is still unclear how the process occurs in detail, several important parameters have been identified: the initial suppression of the crystallization of PFDMS, and the fact that the selective co-solvent has to be added within a fairly narrow time window. After vesicle formation, the crystallinity and rigidity of PFDMS seems to be beneficial for capsule stabilization.[64] The incorporation of a PAG, on the other hand, demonstrated a means to achieve controlled degradation and the potential release of an encapsulated "cargo". An interesting feature of this work is that the star-block copolymers employed are moderately polydisperse. Future studies will also focus on the study of comparable, but less polydisperse systems in which both arm number and length are well-defined. This would help clarify whether the reported self-assembly behavior can be ascribed solely to the star-shaped architecture or if the polydispersity of the system has a key role, as has previously been identified in vesicle formation by linear diblock copolymers.[65]

Experimental Section

Materials: All solvents used for self-assembly studies were purchased in analytical grade from Aldrich and used as received. Solvents for polymerization and monomer syntheses were distilled and either freshly used or stored in a glovebox under an argon atmosphere. Karstedt's catalyst was purchased from Genessee Inc. and stored in a fridge at −40 °C in the glovebox. Chloro(methyl)phenylsilane and the photoacid generator, 2-(4-methoxystyryl)-4,6-bis(trichloromethyl)-1,3,5-triazine, were obtained from Aldrich and used as received. The star-shaped, hydroxyl-terminated, poly(ethylene oxide) precursor ($[PEO_{50}]_4$) was purchased from Polymer-Source Inc. The oxidant $[NO][SbF_6]$ was acquired from Aldrich and used as received. $[Fe(C_5H_5)_2][BF_4]$ was purchased from Aldrich and purified following a literature procedure[1] before use. Tris(4-bromophenyl)ammonium hexafluoroantimonate ($[N(C_6H_4Br\text{-}4)_3][SbF_6]$) was synthesized according to a literature protocol[2] and stored in a glovebox at −40 °C.

Monomer synthesis, $Fe(\eta\text{-}C_5H_4)_2SiMe_2$: FDMS (ferrocenyldimethylsilane) was synthesized according to earlier published protocols[3] and purified through three successive recrystallization/sublimation cycles.

$[(PEO)_{50}$-OSiMePhH$]_4$: $[(PEO)_{50}\text{-}OH]_4$ (250 mg, 0.028 mmol) was dissolved in dry toluene (10 mL) at 40 °C. After cooling to room temperature, pyridine (0.57 mmol, 50 μL, 20 equiv) and chloro(methyl)phenylsilane (0.14 mmol, 25 μL, 5 equiv) were added and the reaction mixture was stirred for 24 h at this temperature. Already after a few minutes, precipitation of pyridine hydrochloride could be observed. The pyridine hydrochloride was removed by filtration and the filtrate was concentrated to approximately 5 mL under vacuum. The solution was subsequently added dropwise to hexane (50 mL) to precipitate the star polymer. The white powder was washed three times with hexane (10 mL) and dried in vacuo. Yield: 240 mg (91 %). ^{29}Si DEPT NMR (79.5 MHz, $J_{Si\text{-}H}=6.7$ Hz, $CDCl_3$): $\delta=-11.1$ ppm (s, O*Si*MePhH); ^{1}H NMR (300 MHz, $CDCl_3$): $\delta=0.40$ (s, SiPh*Me*), 3.41 (s, $C(CH_2(OCH_2CH_2)_n)_4$), 3.64 (s, $(OCH_2CH_2)_n$), 5.10 (m, Si*H*), 7.37 (m, Si*Ph*MeH), 7.52 ppm (m, Si*Ph*MeH).

$[PEO_{50}$-*b*-$PFDMS_{35}]_4$: $[(PEO_{50})\text{-}OSiMePhH]_4$ (60 mg. 0.007 mmol) and FDMS (90 mg, 0.372 mmol, ratio 50:1) were dissolved in dry toluene (5 mL) at 40 °C. Then Karstedt's catalyst ((5 μL, 0.4 μmol; 2.1–2.4 % Pt in xylene) was added and the mixture was stirred for 72 h at room temperature. During this time, the color of the reaction mixture changed from red to amber, indicating the consumption of the FDMS monomer. The polymer was precipitated in hexane (50 mL) to yield a yellow powder. Afterwards, the polymer was washed with aliquots of hexane (3×20 mL) and dried in vacuo. Yield: 139 mg (93 %)

Purification: To remove any unreacted $[(PEO_{50})\text{-}OSiMePhH]_4$, the polymer was dissolved in toluene (12 mL) at 40 °C and then kept in the fridge at 0 °C for 24 h, which led to the precipitation of the PEO precursor. The supernatant toluene was added dropwise to hexane (20 mL) to precipitate the polymer (yellow powder), which was subsequently dried in vacuo. Yield: 78 mg (56 %). ^{29}Si DEPT NMR (79.5 MHz, $J_{Si\text{-}H}=6.7$ Hz, $CDCl_3$): $\delta=-6.3$ ppm (s, *Si*Me$_2$); ^{1}H NMR (300 MHz, $CDCl_3$): $\delta=0.31$ (s, SiPh*Me*), 0.45 (s, FcSi*Me*$_2$), 3.41 (s, $C(CH_2(OCH_2CH_2)_n)_4$), 3.64 (s, $(OCH_2CH_2)_n$), 4.01 (m, *Cp*), 4.21 (m, *Cp*), 7.35 (m, Si(*Ph*Me)O), 7.63 ppm (m, Si(*Ph*Me)O). Integration gave a ratio of 5.66 (3.64 ppm, 4H, CH_2CH_2, PEO) to 6 (0.45 ppm, 6H, $SiMe_2$, PFDMS), resulting in PEO/PFDMS = 1.42:1.

$[PEO_{50}$-*b*-$PFDMS_{30}]_4$ ($M_n=37\,800$ g mol^{-1}; PDI = 1.39; PEO/PFDMS = 1.65:1) and $[PEO_{50}$-*b*-$PFDMS_{16}]_4$ ($M_n=24\,300$ g mol^{-1}; PDI = 1.41; PEO/PFDMS = 3.1:1) were synthesized using the same protocol as described for $[PEO_{50}$-*b*-$PFDMS_{35}]_4$ and with the corresponding amounts of educts.

Encapsulation of 2-(4-methoxystyryl)-4,6-bis(trichloromethyl)-1,3,5-triazine (PAG): $[PEO_{50}$-*b*-$PFDMS_{35}]_4$ (2 mg) and the PAG (2 mg) were dissolved in THF (2 mL). Afterwards, EtOH (4 mL) was added within 1 min to induce self-assembly and encapsulation of the PAG. "Free" PAG was removed by five successive dialysis steps against pure EtOH. After the last step, first TEM was used to confirm that the vesicles are intact prior to UV irradiation (Figure S5).

Partial oxidation of PFDMS in solution: Solutions of $[PEO_{50}$-*b*-$PFDMS_{35}]_4$ in THF/EtOH (1:2, v/v) were degassed by nitrogen bubbling for 10 min. Stock solutions of any oxidizing agent ($[Fe(C_5H_4)_2][BF_4]$, $[N(C_6H_4Br)_3][SbF_6]$, $[NO][SbF_6]$) were prepared in a glovebox using freshly distilled THF (5 g L^{-1}) and sealed with a septum. The respective amount of oxidating agent was then added to the degassed vesicle solution with a flushed syringe using Schlenk techniques.

Polymer characterization: Size exclusion chromatography (SEC) was carried out by using a Viscotek VE 2001 Triple-Detector gel permeation chromatograph equipped with an automatic sampler, a pump, an injector, an inline degasser, and a column oven (30 °C). The elution columns consisted of styrene/divinylbenzene gels with pore sizes of 500 and 100 000 Å. Detection was conducted by using a VE 3580 refractometer, a four-capillary differential viscometer, and a 90° and low-angle (7°) laser light ($\lambda_0=670$ nm) scattering detector (VE 3210 and VE 270). THF (Fisher) was used as the eluent at a flow rate of 1.0 mL min^{-1}. Samples were dissolved in the eluent (2 mg mL^{-1}) and filtered with a Ministart SRP 15 filter (poly(tetrafluoroethylene) membrane of 0.45 μm pore size)

before analysis. The calibration was conducted by using a PolyCAL™ polystyrene standard (PS115K) from Viscotek.

To determine the molecular weight of the star-shaped block copolymers obtained, the molecular weight M_n of the first block from SEC measurements was compared with the block ratio of the diblock copolymer obtained by integrating the ^{1}H NMR spectroscopy signal intensities of the respective blocks. The characteristics of the star-block copolymers are listed in Table 1.

Dialysis: Dialysis membrane tubing (MWCO 8000–12000 g mol^{-1}, regenerated cellulose ester) were purchased from Spectra/Por. Prior to use, the tubes were immersed in deionized water for 30 min to open the pores.

Vesicle preparation: The star-shaped block copolymers were dissolved in THF at a concentration of 1 g L^{-1} and these solutions served as stock. Addition of selected solvents (MeOH, EtOH, *n*BuOH) was either performed at once with a syringe in different ratios or over time (mentioned within the manuscript where appropriate) using a KdS 100 syringe pump at different dosing rates. The samples were mechanically stirred during the addition of the selective solvent.

Dynamic light scattering (DLS): DLS (173°) experiments were performed using a nano series Malvern zetasizer instrument equipped with a 633 nm red laser. Samples were analyzed in 1 cm glass cuvettes at 25 °C. The refractive indices of the block copolymers involved were assumed to be 1.60. DLS results are reported as apparent hydrodynamic radii ($R_{H,app}$), acknowledging that the particles have been modeled as spheres in the experiments conducted. Prior to measurement, the samples were filtered through 5 μm PTFE syringe filters.

Angular-dependent dynamic light scattering: DLS was performed at a scattering angle of 90° or at multiple angles ranging from 30–150° in 10° steps on an ALV CGS-3 instrument and a He–Ne laser operating at a wavelength of $\lambda = 633$ nm. The CONTIN algorithm was applied to analyze the correlation functions obtained. Apparent hydrodynamic radii were calculated according to the Stokes–Einstein equation. All CONTIN plots are intensity-weighted. Samples were prepared as described above in mixtures of THF/ethanol (1:2, v/v).

Static light scattering (SLS): SLS was performed using an ALV CGS-3 goniometer system equipped with a He—Ne laser operating at 633 nm at 25 °C. Samples were prepared as described above in mixtures of THF/ethanol (1:2, v/v) and dialyzed against pure ethanol. The refractive index increment (dn/dc) was determined using six different concentrations (0.033, 0.066, 0.132, 0.198, 0.264, and 0.33 g L^{-1}). These were filtered through 1.5 μm Nylon syringe filters and subsequently measured at scattering angles in the range of 25 to 150° in steps of 5°. The data was evaluated using a Berry plot with the ALVStat program.

Wide-angle-X-ray scattering (WAXS): X-ray powder diffraction data were collected with $Cu_{K\alpha}$ radiation ($\lambda = 1.5418$ Å) on a Bruker D8 Advance powder diffractometer fitted with a 0.6 mm fixed divergence slit, knife-edge collimator, and a LynxEye area detector. Data were collected between $2\theta = 3$–40° in $\theta/2\theta$ mode.

Scanning electron microscopy (SEM): SEM images were obtained by using a Hitachi S-4500 field-emission scanning electron microscope operating at 1.0 kV.

Transmission electron microscopy (TEM): TEM copper grids from Agar Scientific, mesh 400, were coated with a carbon film. Carbon coating was carried out using an Agar TEM Turbo Carbon Coater, the carbon being sputtered onto mica sheets before deposition on to the grids by means of flotation.

The samples for electron microscopy were prepared by drop casting one drop (ca. 50 μL) of the micelle solution onto a carbon-coated copper grid, which was placed on a piece of filter paper to remove excess solvent. Bright field TEM micrographs were obtained on a JEOL1200EX microscope operating at 120 kV and equipped with an SIS MegaViewIII digital camera. No staining of the images was necessary.

Cryogenic transmission electron microscopy (cryo-TEM): The samples were rapidly frozen in liquid ethane using an FEI Vitrobot plunge freezing device and analyzed by using a 200 kV FEI Tecnai 20 LaB6 TEM equipped with a Gatan 626 Cryo transfer holder. The microscope was optimized for cryo applications with additional cryoblades and low dose software. The images were taken on an FEI Eagle 4K × 4K camera.

For cryo-TEM in mixtures of THF/ethanol, 2 μL of the respective sample solution were applied to a copper grid covered with a holey carbon film (Quantifoil R3.5/1 Micro Tools GmbH, Jena, Germany). Excess sample was blotted automatically with filter paper (1 s) and samples were then rapidly plunged into liquid ethane (cooled to about −180 °C) in a cryobox (Carl Zeiss NTS, GmbH). After removing excess ethane with a filter paper, the samples were transferred with a cryo-transfer unit (Gatan 626-DH, Gatan GmbH, Munich, Germany) into the precooled cryo-electron microscope operating at 120 kV (Philips CM 120, Eindhoven, Netherlands) and viewed under low dose conditions with a bottom-mounted 1k CCD camera.

Surface probe microscopy (SPM): All AFM images were obtained by using a Multimode atomic force microscope equipped with a Nanoscope V controller (Veeco Instruments Ltd, Santa Barbara, USA). Samples were spin-cast onto silicon wafers from 0.1 mg mL^{-1} solutions in the respective solvent mixture. Images were taken in air at ambient temperature. Image analysis was carried out by using Gwyddion, an open source software program for SPM images (www.gwyddion.net).

UV irradiation: UV irradiation was performed with a UVA-Cube 100 (mercury lamp; $\lambda \cong 320$–400 nm) purchased from Dr. Hönle AG (München, Germany).

Acknowledgements

The authors thank the European Union for financial support. F.H.S. (DAAD) and S.K.P. (European Union, Marie Curie) are grateful for postdoctoral fellowships. I.M. thanks the European Union for a Marie Curie Chair, the European Research Council for an Advanced Investigator Award and the Royal Society for a Wolfson Merit Award. We thank John A. Jones for the SEM measurements, Judith Mantell for help with the cryo-TEM experiments and Florian Wieberger (Universität Bayreuth) for helpful discussions. We also thank Thomas Lunkenbein and Josef Breu (Universität Bayreuth) for temperature-dependent WAXS measurements and discussions. M.A.W. thanks NSERC for support. F.H.S. also thanks the Thuringian Ministry for Education, Science, and Culture (TMBWK; grants B514-09051, NanoConSens, and B515-10065, ChaPoNano) for financial support.

[1] I. W. Hamley, *Angew. Chem.* **2003**, *115*, 1730–1752; *Angew. Chem. Int. Ed.* **2003**, *42*, 1692–1712.
[2] V. Abetz, P. F. W. Simon, *Adv. Polym. Sci.* **2005**, *189*, 125–212.
[3] H.-C. Kim, S.-M. Park, W. D. Hinsberg, *Chem. Rev.* **2010**, *110*, 146–177.
[4] J.-F. Gohy, *Adv. Polym. Sci.* **2005**, *190*, 65–136.
[5] K. Matyjaszewski, N. V. Tsarevsky, *Nat. Chem.* **2009**, *1*, 276–288.
[6] G. R. Whittell, I. Manners, *Adv. Mater.* **2007**, *19*, 3439–3468.
[7] J. Yun, R. Faust, L. S. Szilágyi, S. Kéki, M. Zsuga, *J. Macromol. Sci. A Pure Appl. Chem.* **2004**, *41*, 613–627.
[8] M. A. C. Stuart, W. T. S. Huck, J. Genzer, M. Müller, C. Ober, M. Stamm, G. B. Sukhorukov, I. Szleifer, V. V. Tsukruk, M. Urban, F. Winnik, S. Zauscher, I. Luzinov, S. Minko, *Nat. Mater.* **2010**, *9*, 101–113.
[9] G. Riess, *Prog. Polym. Sci.* **2003**, *28*, 1107–1170.
[10] C.-H. Lin, W.-C. Chen, H.-L. Chen, *Macromol. Chem. Phys.* **2008**, *209*, 2349–2358.
[11] D. Fournier, R. Hoogenboom, H. M. L. Thijs, R. M. Paulus, U. S. Schubert, *Macromolecules* **2007**, *40*, 915–920.
[12] F. A. Plamper, A. Schmalz, A. H. E. Müller, *J. Am. Chem. Soc.* **2007**, *129*, 14538–14539.
[13] D. A. Rider, M. A. Winnik, I. Manners, *Chem. Commun.* **2007**, 4483–4485.
[14] F. A. Plamper, L. Murtomaki, A. Walther, K. Kontturi, H. Tenhu, *Macromolecules* **2009**, *42*, 7254–7257.

[15] F. Schacher, A. Walther, A. H. E. Müller, *Langmuir* **2009**, *25*, 10962–10969.
[16] P. S. Chelushkin, E. A. Lysenko, T. K. Bronich, A. Eisenberg, V. A. Kabanov, A. V. Kabanov, *J. Phys. Chem. B* **2008**, *112*, 7732–7738.
[17] J. B. Gilroy, T. Gädt, G. R. Whittell, L. Chabanne, J. A. Mitchels, R. M. Richardson, M. A. Winnik, I. Manners, *Nat. Chem.* **2010**, *2*, 566–570.
[18] M. Lazzari, D. Scalarone, C. Vazquez-Vazquez, M. A. Lòpez-Quintele, *Macromol. Rapid Commun.* **2008**, *29*, 352–357.
[19] Z.-X. Du, J.-T. Xu, Z.-Q. Fan, *Macromol. Rapid Commun.* **2008**, *29*, 467–471.
[20] C.-K. Chen, S.-C. Lin, R.-M. Ho, Y.-W. Chiang, B. Lotz, *Macromolecules* **2010**, *43*, 7752–7758.
[21] X. Wang, G. Guerin, H. Wang, Y. Wang, I. Manners, M. A. Winnik, *Science* **2007**, *317*, 644–647.
[22] H. Wang, M. A. Winnik, I. Manners, *Macromolecules* **2007**, *40*, 3784–3789.
[23] H. Schmalz, J. Schmelz, M. Drechsler, J. Yuan, A. Walther, K. Schweimer, A. M. Mihut, *Macromolecules* **2008**, *41*, 3235–3242.
[24] V. Bellas, M. Rehahn, *Angew. Chem.* **2007**, *119*, 5174–5197; *Angew. Chem. Int. Ed.* **2007**, *46*, 5082–5104.
[25] T. Gädt, N. S. Ieong, G. Cambridge, M. A. Winnik, I. Manners, *Nat. Mater.* **2009**, *8*, 144–150.
[26] S. Strandman, S. Hietala, V. Aseyev, B. Koli, S. J. Butcher, H. Tenhu, *Polymer* **2006**, *47*, 6524–6535.
[27] S. Strandman, A. Zarembo, A. A. Darinskii, P. Laurinmäki, S. J. Butcher, E. Vuorimaa, H. Lemmetyinen, H. Tenhu, *Macromolecules* **2008**, *41*, 8855–8864.
[28] S. Hietala, P. Mononen, S. Strandman, P. Järvi, M. Torkkeli, K. Jankova, S. Hvilsted, H. Tenhu, *Polymer* **2007**, *48*, 4087–4096.
[29] M. R. Whittaker, M. J. Monteiro, *Langmuir* **2006**, *22*, 9746–9752.
[30] M. Libera, W. Walach, B. Trzebicka, S. Rangelov, A. Dworak, *Polymer* **2011**, *52*, 3526–3536.
[31] C. Liu, M. A. Hillmyer, T. P. Lodge, *Langmuir* **2009**, *25*, 13718–13725.
[32] Z. Iatridi, C. Tsitsilianis, *Chem. Commun.* **2011**, *47*, 5560–5562.
[33] I. Korczagin, M. A. Hempenius, R. G. Fokkink, M. A. Cohen Stuart, M. Al-Hussein, P. H. H. Bomans, P. M. Frederik, G. J. Vancso, *Macromolecules* **2006**, *39*, 2306–2315.
[34] M. Lazzari, M. A. López-Quintela, *Macromol. Rapid Commun.* **2009**, *30*, 1785–1791.
[35] F. Wurm, S. Hilf, H. Frey, *Chem. Eur. J.* **2009**, *15*, 9068–9077.
[36] T. Gädt, F. H. Schacher, N. McGrath, M. A. Winnik, I. Manners, *Macromolecules* **2011**, *44*, 3777–3786.
[37] E. K. Lin, A. P. Gast, *Macromolecules* **1996**, *29*, 4432–4441.
[38] A. T. Lorenzo, A. J. Müller, M.-C. Lin, H.-L. Chen, U. S. Jeng, D. Priftis, M. Pitsikalis, N. Hadjichristidis, *Macromolecules* **2009**, *42*, 8353–8364.
[39] R. H. Jin, *Macromol. Chem. Phys.* **2003**, *204*, 403–409.
[40] J. A. Massey, K. Temple, L. Cao, Y. Rharbi, J. Raez, M. A. Winnik, I. Manners, *J. Am. Chem. Soc.* **2000**, *122*, 11577–11584.
[41] P. Gómez-Elipe, R. Resendes, P. M. Macdonald, I. Manners, *J. Am. Chem. Soc.* **1998**, *120*, 8348–8356.
[42] R. Resendes, J. A. Massey, K. Temple, L. Cao, K. N. Power-Billard, M. A. Winnik, I. Manners, *Chem. Eur. J.* **2001**, *7*, 2414–2424.
[43] R. Resendes, J. Massey, H. Dorn, M. A. Winnik, I. Manners, *Macromolecules* **2000**, *33*, 8–10.
[44] J. Rasburn, R. Petersen, T. Jahr, R. Rulkens, I. Manners, G. J. Vancso, *Chem. Mater.* **1995**, *7*, 871–877.
[45] R. G. H. Lammertink, M. A. Hempenius, I. Manners, G. J. Vancso, *Macromolecules* **1998**, *31*, 795–800.
[46] J. Gwyther, I. Manners, *Polymer* **2009**, *50*, 5384–5389.
[47] K. Temple, F. Jäkle, J. B. Sheridan, I. Manners, *J. Am. Chem. Soc.* **2001**, *123*, 1355–1364.
[48] W. Burchard, *Adv. Polym. Sci.* **1983**, *48*, 1–124.
[49] H. Cui, T. K. Hodgdon, E. W. Kaler, L. Abezgauz, D. Danino, M. Lubovsky, Y. Talmon, D. J. Pochan, *Soft Matter* **2007**, *3*, 945–955.
[50] H. Friedrich, P. M. Frederik, G. de With, N. A. J. M. Sommerdijk, *Angew. Chem.* **2010**, *122*, 8022–8031; *Angew. Chem. Int. Ed.* **2010**, *49*, 7850–7858.
[51] G. T. Oostergetel, F. J. Esselink, G. Hadziioannou, *Langmuir* **1995**, *11*, 3721–3724.
[52] F. Schacher, A. Walther, M. Ruppel, M. Drechsler, A. H. E. Müller, *Macromolecules* **2009**, *42*, 3540–3548.
[53] Y. Yu, L. Zhang, A. Eisenberg, *Langmuir* **1997**, *13*, 2578–2581.
[54] Y. Yu, A. Eisenberg, *J. Am. Chem. Soc.* **1997**, *119*, 8383–8384.
[55] K. H. Pannell, V. V. Dementiev, H. Li, F. Cervantes-Lee, M. T. Nguyen, A. F. Diaz, *Organometallics* **1994**, *13*, 3644–3650.
[56] We are further investigating this issue. Initial WAXS experiments at 150 °C (above the melting point of linear PFDMS (145 °C)) show that the reflections observed at $2\theta = 7.3$ and 12.15° disappear. This provides support for the assertion that these signals can be ascribed to the PFDMS part of the star-block copolymer aggregates.
[57] A. Ranquin, W. Versèes, W. Meier, J. Steyaert, P. Van Gelder, *Nano Lett.* **2005**, *5*, 2220–2224.
[58] D. E. Discher, A. Eisenberg, *Science* **2002**, *297*, 967–973.
[59] We have recently prepared redox-active vesicles by the self-assembly of amorphous PFDMS-*b*-PDMS diblock copolymers in which the PFDMS segment is a polyelectrolyte, see: K. N. Power-Billard, R. J. Spontak, I. Manners, *Angew. Chem.* **2004**, *116*, 1280–1284; *Angew. Chem. Int. Ed.* **2004**, *43*, 1260–1264.
[60] G. Pohlers, J. C. Scaiano, R. Sinta, R. Brainard, D. Pai, *Chem. Mater.* **1997**, *9*, 1353–1361.
[61] A. Napoli, M. J. Boerakker, N. Tirelli, R. J. M. Nolte, N. A. J. M. Sommerdijk, J. A. Hubbell, *Langmuir* **2004**, *20*, 3487–3491.
[62] E. Mabrouk, D. Cuvelier, F. Brochard-Wyart, P. Nassoy, M.-H. Li, *Proc. Natl. Acad. Sci. USA* **2009**, *106*, 7294–7298.
[63] Y. Ma, W.-F. Dong, M. A. Hempenius, H. Möhwald, G. J. Vancso, *Nat. Mater.* **2006**, *5*, 724–729.
[64] Preliminary studies with an amorphous organometallic block copolymer lead to similar structures, but with a distinctly reduced stability. This will be the subject of a forthcoming publication.
[65] L. Luo, A. Eisenberg, *J. Am. Chem. Soc.* **2001**, *123*, 1012–1013.

Received: July 27, 2011
Published online: December 9, 2011

